JOURNAL OF GEOPHYSICAL RESEARCH, VOL. 108, NO. C12, 8136, doi:10.1029/2001JC001252, 2003

EBENE: A JGOFS investigation of plankton variability and trophic interactions in the equatorial Pacific (180°)

Robert Le Borgne
Institut de Recherche pour le Développement, Centre de Nouméa, New Caledonia

Michael R. Landry
Department of Oceanography, University of Hawaii at Manoa, Honolulu, Hawaii, USA

Received 11 December 2001; revised 5 January 2003; accepted 21 January 2003; published 17 October 2003.

[1] The Etude du Broutage en Zone Equatoriale (EBENE) transect (8°S–8°N) explored the equatorial high-nutrient, low-chlorophyll (HNLC) zone and adjacent oligotrophic areas during a La Niña period (October–November 1996). During this time the passage of a tropical instability wave also influenced the region north of the equator. We present a brief summary of EBENE findings, with an emphasis on phytoplankton utilization by the assemblage of protistan and animal consumers. Despite significant variability over the diel cycle, phytoplankton biomass at the equator was relatively constant on a 24-hour timescale, denoting a dynamic balance between growth and losses. The magnitude of the daily cycle in phytoplankton biomass was well constrained by in situ observations of the diel variability in pigments and suspended particulates, by ^{14}C uptake rates from in situ incubations, and from experimental determinations of specific growth and grazing rates. The general equilibrium of production and grazing processes is illustrated by applying biomass-specific grazing rates from the equatorial station to measured planktonic biomass along the EBENE transect and comparing them to measured ^{14}C uptake. Most of the grazing turnover is supported by the production of *Prochloroccus* (31%) and picoeukaryotic algae (34%). Among the consumers, microzooplankton (<200 μm) account for 59–98% of the grazing losses. The coherence of the results obtained by independent methods suggests that the essential features of the system have been adequately represented by rate and standing stock assessments from the EBENE study. *INDEX TERMS:* 4231 Oceanography: General: Equatorial oceanography; 4805 Oceanography: Biological and Chemical: Biogeochemical cycles (1615); 4815 Oceanography: Biological and Chemical: Ecosystems, structure and dynamics; 4855 Oceanography: Biological and Chemical: Plankton; 4817 Oceanography: Biological and Chemical: Food chains; *KEYWORDS:* equatorial Pacific, plankton, grazing, growth, diel cycle

Citation: Le Borgne, R., and M. R. Landry, EBENE: A JGOFS investigation of plankton variability and trophic interactions in the equatorial Pacific (180°), *J. Geophys. Res.*, *108*(C12), 8136, doi:10.1029/2001JC001252, 2003.

1. Introduction

[2] The equatorial Pacific divergence is the world's largest and most seasonally consistent source of upwelled waters to the surface ocean. As such, it is both the main natural source of carbon dioxide from the oceans [*Feely et al.*, 2002] and one of its major regions of new production [*Chavez and Togweiler*, 1995]. In contrast with coastal upwelling regions, equatorial surface waters are marked by persistently elevated concentrations of macronutrients, indicating disequilibrium between their inputs and uptake by primary production. On the global scale, the geographical distributions of macronutrients and plankton concentrations are notably decoupled in this high-nutrient, low-chlorophyll (HNLC) system [*Minas et al.*, 1986; *Le Borgne et al.*, 2002a].

[3] In the earliest explanation for the low phytoplankton biomass levels in the equatorial upwelling region, *Walsh* [1976] speculated that low-frequency variability of hydrographical variables allowed for a balanced existence of prey and predators. Indeed, many studies have documented a remarkable steadiness of equatorial plankton abundances and biomass even while showing considerable dynamics over the diel cycle [see *Binder and DuRand*, 2002]. Nonetheless, *Walsh*'s [1976] explanation did not consider population-specific differences in responses and regulation within the assemblage of phytoplankton prey and zooplankton grazers. In addition, it predated major discoveries relating to the microbial food web interactions and picophytoplankton dominance in the tropical open oceans [e.g., *Azam et al.*, 1983; *Chisholm et al.*, 1988]. Protistan control of picophyplankton and nanophytoplank-

0148-0227/03/2001JC001252$09.00

ton is now recognized as integral to the explanation of the HNLC condition of relatively low and constant concentrations of fast growing phytoplankton [*Cullen et al.*, 1992; *Frost and Franzen*, 1992; *Price et al.*, 1994; *Landry et al.*, 2000a]. At the same time, iron availability exerts strong bottom-up influence on plankton growth rates and total biomass accumulation [*Morel et al.*, 1991; *Coale et al.*, 1996; *Landry et al.*, 1997]. Iron limitation effects are seen in the variability of larger phytoplankton cells, which are controlled less efficiently by mesozooplankton grazers [*Landry et al.*, 2000b]. Moreover, *Blain et al.* [1997] and *Dugdale and Wilkerson* [1998] have pointed to the role of silicate in limiting populations of diatoms and other siliceous plankton.

[4] Top-down and bottom-up controls may also show some latitudinal dependencies. Iron inputs, for example, are expected to be maximum on the equator because of their source in upwelled water from the Equatorial Undercurrent (EUC) [*Gordon et al.*, 1997]. Similarly, the pathways of top-down control may vary with latitude as the trophic structure evolves and matures with poleward advection within the HNLC region. While several modeling studies of the HNLC ecosystem have simulated variable iron [*Leonard et al*, 1999; *Friedrichs and Hofmann*, 2001] and silicate inputs [*Chai et al.*, 2002] in order to consider their food web impacts, there still is a need for comprehensive field observations to define community and food web structures, test mechanisms and provide real data constraints on our understanding.

[5] The nine papers that follow in this Special Section present the detailed results of Etude du Broutage en Zone Equatoriale, Study of Grazing In the Equatorial Zone (EBENE), a component of France-Joint Global Ocean Flux Study (JGOFS) and part of the JGOFS equatorial Pacific field program. EBENE research was conducted on a cruise aboard the R/V *L'Atalante* (21 October to 20 November 1996) with the goals of providing a more coherent understanding of diel cycles and latitudinal scales of variability in the equatorial region and their links to phytoplankton production and zooplankton grazing processes. Various components of this study provide the first report of physical and ecological effects of a tropical instability wave as far west as 180°, the first comprehensive study of plankton community biomass structure (bacteria to mesozooplankton) across the equatorial region, plankton size fraction influences on bio-optical properties of the surface layer, latitudinal variations in marine snow distributions to 1000 m depth, and complementary observational and experimental assessments of the magnitude of the phytoplankton daily production cycle and its utilization by the assemblage of protistan and animals consumers. In this brief introduction to EBENE findings, we emphasize, in particular, this latter theme by bringing together data relating to the daily balance of growth and grazing processes.

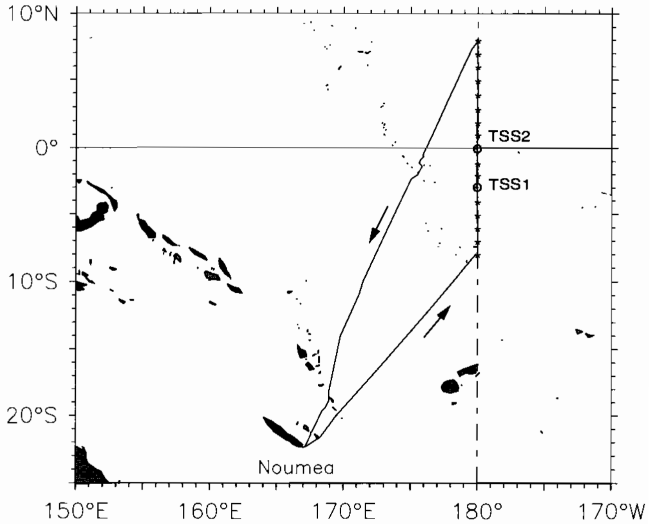

Figure 1. Track of the EBENE cruise (21 October to 20 November 1996) on board R/V *L'Atalante*. The transect from 8°S to 8°N consisted of short stations made every degree of latitude and two 5-day time series stations, TSS1 and TSS2.

2. EBENE Cruise Plan

[6] The EBENE cruise plan involved two main activities: sampling of latitudinal variability along a cross-equatorial transect from 8°S to 8°N, 180° and 5-day diel studies of plankton variability and process rates at two time series stations, 3°S (TSS1) and the equator (TSS2) (Figure 1). The transect was sampled at every degree of latitude (17 stations) for hydrographic variables, in vivo fluorescence, transmissometry, PAR (Photosynthetic Available Radiation), nutrients, spectrofluorometric pigments, flow cytometric and microscopical analyses for population abundances and biomass of picoplankton, nanoplankton, and microplankton, net tows for mesozooplankton and vertical profiles made with a video camera system to examine macroparticle distributions in the water column to 1000 m. In addition, water collected at 20-m depth at each station was used in shipboard ^{14}C uptake experiments to assess the latitudinal pattern in maximum mixed layer photosynthesis.

[7] Diel studies at TSS1 and TSS2 began with 48 hours of hourly CTD rosette sampling (0–150 m) of hydrographic variables, nutrients, pigments and flow cytometric populations. This was followed by a 48-hour focus on the mesozooplankton component, consisting of sampling at 3-hour intervals with different nets for biomass, metabolic rates (feeding, respiration and excretion), and gut fluorescence measurements. Over the course of the diel sampling, experimental studies were conducted to assess taxon-specific rates of phytoplankton growth and micrograzer impact at 30 and 60 m, and uptake rates of ^{14}C, ^{15}N and ^{32}Si were determined from in situ incubations of 6, 12 and/or 24 h. Lastly, vertical profiles were made with the video camera system. Detailed descriptions of the methodologies and resulting data are found in the accompanying papers in this volume and in cruise reports by *Le Borgne et al.* [1998] and *Le Borgne* [1999].

3. General Oceanographic Conditions During EBENE

[8] By circumstance rather than design, EBENE coincided with the cold-phase conditions (La Niña) of an ENSO

cycle [*Eldin and Rodier*, 2003]. This was reflected in Polder-ADEOS sea color images from 1–10 November 1996 [*Dupouy et al.*, 2003] which showed the HNLC zone extending west of 180°, and as far as 165°E, during the cruise. This situation was the consequence of trade winds having been above average in the equatorial waveguide (i.e., 2°S–2°N) from the first quarter to November 1996. Data from the TAO mooring array (http://www.pmel.noaa.gov/tao) also indicated a slight sea surface cooling and 10-m deepening of the thermocline on 180°. Such observations indicated an active upwelling with a wedge-shaped tongue penetrating waters of the warm pool.

[9] As in previous equatorial transects [*Murray et al.*, 1995], nitrate and phosphate distributions from EBENE were asymmetrical with respect to the equator, with surface nitrate and phosphate concentrations being above 0.1 and 0.3 μM, respectively, between 7°S and 5°N. A similar pattern was evident for integrated total chlorophyll *a* (Tchl *a*). This latitudinal range encompasses two convergence zones around 6°S and 4°N, and represents the extent of the HNLC area as visualized in Polder-ADEOS sea color images [*Dupouy et al.*, 2003]. Asymmetry was also observed in microbial biomass and community composition [*Brown et al.*, 2003], which were used to calibrate sea color images and to interpret absorption and backscattering coefficients [*Dupouy et al.*, 2003].

[10] In contrast to the higher surface concentrations of nitrate and phosphate south of the equator, silicate distribution was symmetrical. The Si/N ratio was <1 in the region between 5°S and 1°S, indicating a decoupling between nitrogen and silica recycling [*Leynaert et al.*, 2001] and diatom iron limitation with surface water advection away from the upwelling source of iron [*Hutchins and Bruland*, 1998]. Interestingly, no such a feature was observed north of the equator. This may be interpreted as the result of different iron inputs, with possibly more aeolian flux occurring north of the equator (D. A. Hutchins, personal communication). According to subsurface maxima in ammonium and nitrite concentrations and biomass peaks of heterotrophic bacteria and mesozooplankton, nitrogen remineralization appeared to be highest between 3°S and 6°S and weaker north of the equator. Asymmetrical rates and indices of remineralization are a common feature of equatorial transects, such as EqPac cruises along 140°W [*Murray et al.*, 1995]. However, the asymmetry in surface nitrate and phosphate was influenced, at least in part on this cruise, by the passage of the rear edge of a tropical instability wave (TIW), with a very low nitrate gradient observed north of the equator over 5° of latitude [*Eldin and Rodier*, 2003].

[11] *Eldin and Rodier* [2003] provide evidence that the southern branch of a TIW reached the equator at the beginning of the equatorial time series station (TSS2), which appears to be the first record to date of their effect as far west as 180°. During TSS2, an abrupt decrease of salinity and NO_3 concentration occurred after the first day, consistent with the TIW frontal structure reaching the equator at this time. In addition, ADCP (Acoustic Doppler Current Profiler) current measurements showed horizontal advection of the upper 80-m layer originating from the NE. This pattern differed from EqPac observations from October 1992, when higher NO_3, chlorophyll *a* and zooplankton concentrations coincided with meridional flow to the north associated with the leading edge of a TIW [*Roman et al.*, 1995; *Foley et al.*, 1997].

4. Temporal Variability at the Time Series Stations

4.1. General Features

[12] TSS1 at 3°S presented a deeply mixed layer (>100 m) with very small temporal fluctuations in nutrient concentrations. High-frequency variability, linked to atmospheric forcing and internal wave activity did not seem to modify nutrient and pigment distributions, and physical influences dominated over biology at this station [*Eldin and Rodier*, 2003].

[13] The situation at TSS2 was different because of advection of fresher and lower nitrate waters from the northeast. However, this advective influence seemed to have only a small effect on the temporal variations of most of the biological parameters between the beginning and the end of TSS2. *Neveux et al.* [2003] reported a larger amplitude of the decreasing phase of the daily chl *a* cycle during the passage of the front, which occurred over a 15-hour period. However, depth-integrated chl *a* and vertical distributions were similar from one day to another, leading to remarkably constant ^{14}C uptake rates: 856 mgC m^{-2} d^{-1} at the beginning versus 833 mgC m^{-2} d^{-1} at the end [*Le Bouteiller et al.*, 2003]. Conversely, a slight increase in ammonium concentration (0.2 μM) during the second half of TSS2 was linked to higher abundance of microbial heterotrophs, leading *Brown et al.* [2003] to suggest that these waters were biologically more mature. Mesozooplankton biomass declined by 40% from the beginning of diel sampling to the end. Since mesozooplankton biomass typically displays a local minimum at the equator with symmetrical local maxima 2°–3° of latitude to either side [*White et al.*, 1995], *Le Borgne et al.* [2003] ascribed this temporal decrease to having sampled first the zone of enhanced zooplankton associated with the passage of the TIW front, followed by decreasing concentrations as more water was advected from the north.

[14] The day-to-day relative constancy of biological parameters has been observed previously during equatorial time series studies, particularly in the western and central Pacific [e.g., *Le Borgne et al*, 2002b]. As noted by *Le Bouteiller et al.* [2003], this implies that "the same biological system must have been simultaneously present elsewhere in wide zonal bands parallel to the equator" since strong zonal currents advect water from as far as 45 km away during 24-hour sampling at a fixed position. In the present study, the passage of a TIW resulted in a slight temporal evolution within the heterotrophic community but with little apparent effect on pigment standing stocks and primary productivity.

4.2. Diel Variability

[15] Light-related temporal variations of the phytoplankton were considered at the equator (TSS2) by *Neveux et al.* [2003]. All parameters examined-spectrofluorometric (extracted) pigments, beam attenuation by particles (c_p), *in vivo* fluorescence (F_{iv}), and flow cytometric determinations of cellular forward scattering and fluorescence-showed significant increasing and decreasing phases over 24-hour

cycles. From the high-resolution (hourly) sampling, phase differences were also readily detectable. In the upper 30 m, for example, chl *a* increased from midnight to an early morning peak, while c_p increased during the daytime, and the F_{iv} cycle was largely opposite to that of extracted pigment. In the 30–70 m layer, however, the cycles were out of phase by 2–4 hour, with maxima at ~1500, 1700, and 1900 for chl *a*, c_p, and F_{iv}, respectively. Within this depth strata, each sampled parameter provided independent estimates of phytoplankton growth rate and presumptive grazing loss, assuming that growth occurred only during the daytime while grazing mortality was uniform over a 24-hour cycle. Rate estimates obtained from these in situ observations varied from ~0.5 to 0.7 d^{-1}, in good agreement with the rates of phytoplankton growth and microzooplankton grazing determined experimentally by the dilution technique [*Landry et al.*, 2003].

[16] Diel variabilities of mesozooplankton biomass, feeding and metabolism showed similar amplitudes at the two time series stations, while gut fluorescence contents presented a somewhat greater amplitude at 3°S (TSS1). In the HNLC equatorial region, mesozooplankton generally display rather low diel variation in biomass, a feature ascribed to the relative scarcity of strongly migrating species [*Le Borgne et al.*, 2003]. Thus the night:day biomass ratio for the 0–100 m water column was equal to 1.1 at TSS1 and 1.2 at TSS2. However, migrations did occur within the euphotic zone. For instance, biomass peaks at 1800 in the 0–1 and 0–50 m depth strata at TSS1, were interpreted as being due to upward migration of animals from the 50–100 m strata.

[17] Copepod feeding and metabolic (respiration, ammonium and phosphate excretions) rates were somewhat higher during the daytime period of active phytoplankton growth [*Gaudy et al.*, 2003]. However, mesozooplankton feeding and metabolic losses, the product of biomass and biomass-specific rates, were relatively constant over the 24-hour cycle because of the compensating effect of slightly higher biomass at night [*Gaudy et al.*, 2003]. A similar pattern was seen for the pigment gut content of copepods and their grazing pressure in the 0–100 m water column at TSS2 [*Champalbert et al.*, 2003]. The grazing pressure, however, was clearly higher at TSS1 during the night, and it was the same for surface-living (neustonic) copepods. Overall, the average grazing pressure exerted by the copepod component of the 0–100 m mesozooplankton at TSS2 was equal to 15.7% d^{-1} of the >3-μm chlorophyll stock [*Champalbert et al.*, 2003].

5. An Equatorial Production and Grazing Budget

[18] From the results of the various EBENE component studies, a comparison can be made between taxon-specific autotrophic production and grazing mortality at the equatorial time series station TSS2. For this, we break the euphotic zone into upper (0–50 m; Figure 2) and lower (50–100 m; Figure 3) depth strata, which follows from the division of the water column for mesozooplankton net sampling.

[19] On the basis of the population distinctions in flow cytometric and microscopical analyses, the autotrophic compartment can be split into photosynthetic bacterial populations (*Prochlorococcus* and *Synechococcus*) and small (<8-μm) and large (>8-μm) eukaryotic algae according to *Brown et al.* [2003]. The <8-μm eukaryotes are dominated numerically by picoeukaryotes (i.e., <2-μm cells), while >8-μm eukaryotes are composed of diatoms, autotrophic dinoflagellates, pelagophytes, and prymnesiophytes, the latter constituting the "Other" category. From Figures 2 and 3, eukaryotes accounted for more than 70% of autotrophic biomass at TSS2. The biomass of heterotrophic bacteria (490 mgC m^{-2} in the 0–50 m layer), was slightly larger than the combined picocyanobacteria, *Prochlorococcus* and *Synechococcus* [*Brown et al.*, 2003]. This biomass is not considered in the present budget which focuses on the balance between the autotrophic carbon production and its losses to grazing processes.

[20] Autotroph production rates (P, mgC m^{-2} d^{-1}) were determined from population or community (chl *a*) estimates of specific growth rates (μ, d^{-1}) from triplicate dilution experiments of 30- and 60-m water samples [*Landry et al.*, 2003]. Growth rates were multiplied times their applicable population or community estimates of carbon biomass (B, mgC m^{-2}) [*Brown et al.*, 2003] to estimate production (i.e., $P = \mu \odot B$). The mean community growth rates for the upper and lower strata were 0.76 d^{-1} and 0.27 d^{-1}, respectively, which bridge in situ-based determinations of 0.51 d^{-1} from 30–70 m chl *a* [*Neveux et al.*, 2003]. Combining the productivity index for ^{14}C uptake at 20 m (7.65 mgC m^{-3} h^{-1} (mg chl *a*)$^{-1}$ m^{-3}) [*Le Bouteiller et al.*, 2003] with the mean C:chl *a* ratio for TSS2 (= 100) [*Brown et al.*, 2003] yields a comparable estimate of specific growth rate (0.65 d^{-1}) for the 12-hour photoperiod. This is slightly less than the dilution estimate of 0.76 d^{-1}, by approximately the amount expected to account for losses of ^{14}C-labeled carbon to grazing and microbial cycling during the incubations [*Laws et al.*, 2000; *Landry et al*, 2003]. As an additional check on the internal consistency of the production rate assessments, the ratio of estimated production in the 0–50 m layer to that in the 0–100 m layer (1121 versus 1355 mgC m^{-2} d^{-1} = 0.827) is essentially identical to the ratio from ^{14}C uptake measurements (0.828) [*Le Bouteiller et al.*, 2003].

[21] Phytoplankton consumption by microzooplankton was calculated similarly to production, by multiplying the population or community estimates of mortality losses to microzooplankton grazers (m, d^{-1}) [*Landry et al.*, 2003] times their corresponding estimates of phytoplankton biomass [*Brown et al.*, 2003]. The grazing contribution of the mesozooplankton community was estimated from independent measurements of gut fluorescence. Clearance rate was determined as the amount of chl *a* grazed (I) divided by the mean chlorophyll concentration in the environment (295 μg chl *a* m^{-3} at TSS2), I being defined as the gut pigment content times the gut clearance rate at 28°C divided by the wet weight, WW [*Champalbert et al*, 2003]. WW was converted into carbon using the DW:WW ratio of 0.16 from *Champalbert et al.* [2003] and the C:DW ratio of 0.37 from *Le Borgne et al.* [2003, Table 1], DW and C being dry weight and carbon biomass, respectively. The resulting biomass-specific clearance rate of 0.0313 m^3 (mgC)$^{-1}$ d^{-1} was multiplied times the copepod biomass density to obtain estimates of phytoplankton community mortality (0.14 and 0.07 d^{-1} for the 0–50 and 50–100 m layers, respectively). We computed the contributions of other mesozooplankton

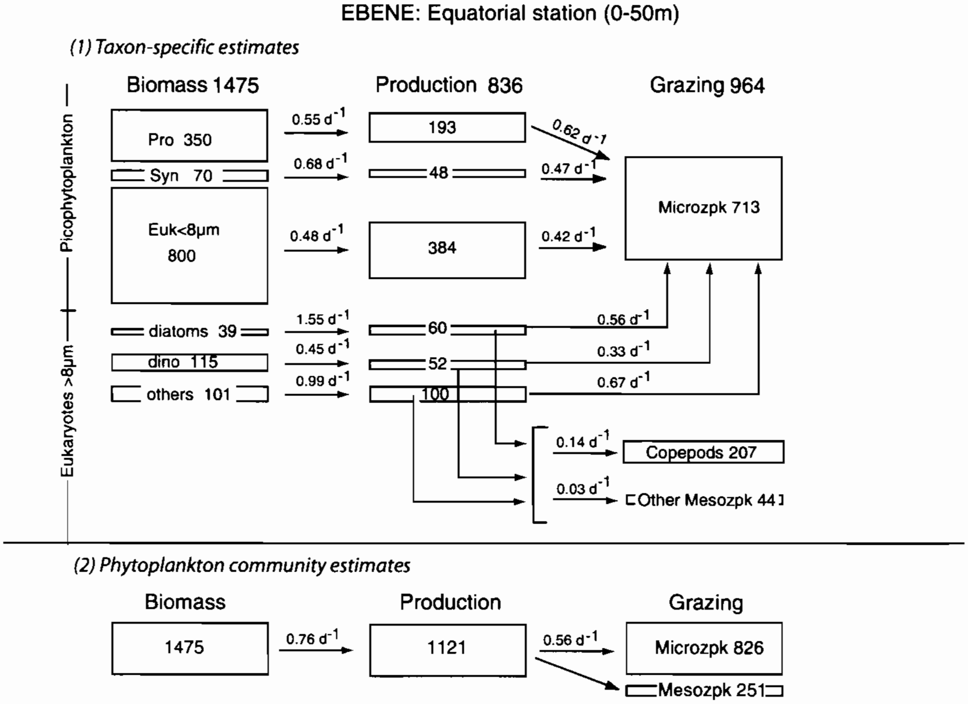

Figure 2. Production and grazing carbon budget of the autotrophic compartment in the 0–50 m layer at equatorial station (TSS2). The upper part of the diagram (1) is based on rate estimates for the different phytoplankton taxa, while the lower one (2) is based on total community estimates from chl *a*. Carbon-based estimates of phytoplankton production and grazing were determined as the product of experimentally determined rates times group-specific or total community biomass. Specific rates of phytoplankton growth, μ (d^{-1}) from *Landry et al.* [2003], are shown above arrows linking phytoplankton biomass and production. Specific rates of microzooplankton grazing (m, d^{-1}) [*Landry et al.*, 2003] are above arrows between production and microzpk grazing. (Picophytoplankton and microzooplankton are from *Brown et al.* [2003]; >8-µm eukaryotes are from M. R. Landry and S. L. Brown (unpublished manuscript); and mesozooplankton are from *Le Borgne et al.* [2003]). Mesozooplankton grazing rates were calculated from *Champalbert et al.* [2003] and *Le Borgne et al.* [2003] as described in the text. Specific rates (above arrows) are applied to the total community chl *a* but are depicted as coming mainly from the larger size fractions. Units are mgC m^{-2} for biomass and mgC m^{-2} d^{-1} for rates.

suspension feeders, mainly euphausiids (9% of total DW), thecosomatous pteropods (3%) and larvaceans (3%) [*Le Borgne et al.*, 2003], assuming their biomass-specific grazing rates were similar to the copepods. This assumption is certainly untrue for larvaceans, which have much higher specific rates [*Gorsky et al.*, 1999], but their impact may be balanced by slower rates for the other taxa. In addition, larvaceans and pteropods may feed on picophytoplankton [*Turner*, 1984; *Deibel and Lee*, 1992] whereas copepods would feed on particles >8 µm [*Gaudy et al.*, 2003]. Given the relatively small contributions of these noncopepod groups to total mesozooplanton biomass, we did not attempt to make corrections reflecting the likely differences in their feeding behaviors.

[22] Comparing the sum of the taxon-specific production rates to the sum of microplankton and mesozooplankton grazing impacts shows an excess of grazing losses over production in the 0–50 m layer (Figure 2(top)), the difference representing ~15% of total production. Within this layer, microzooplankton grazing consumed all production of the picophytoplankton populations and part of the >8-µm eukaryotes, accounting for 74% of total grazing. A better balance between production and grazing losses was found for total "community" rates on the basis of chl *a*, the difference being 4% of total production (Figure 2(bottom)). The inverse was observed for the 50–100 m layer (Figure 3) with a smaller difference (5% of the production) when the sum of production versus grazing losses of the different taxa were considered, while the difference was greater (11%) when community rates were used. Although such small differences may be considered insignificant, they could be ascribed to other unmeasured losses, such as grazing by >2-mm planktonic animals or marine snow formed from flocking phytoplankters (such as diatoms). In this latter regard, *Gorsky et al.* [2003] estimated the marine snow biomass as being about half that of the microbial community and twice that of the mesozooplankton during EBENE. From marine snow vertical and latitudinal distributions, a portion of that formed in the photic layer of TSS2 appears to be exported poleward, sinking in the southern and northern equatorial convergences and returning to the deep layers underneath the equator by the deep circulation.

[23] The present results provide the first assessment of the growth and grazing balance in the equatorial Pacific to consider the contributions of various phytoplankton taxa and grazer groups. They support the idea that despite

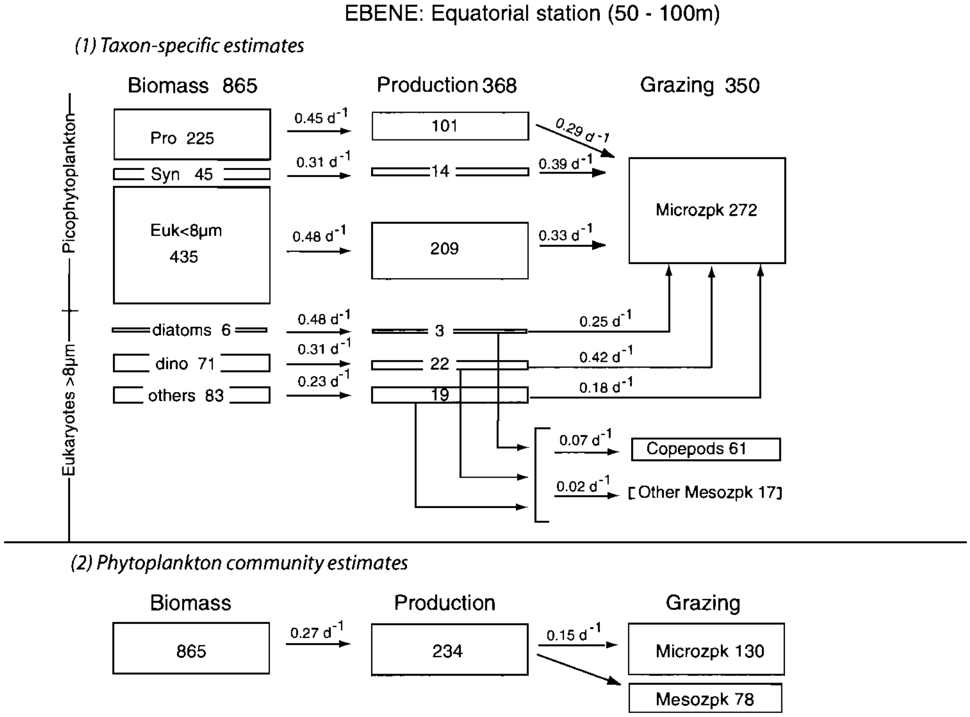

Figure 3. Production and grazing carbon budget of the autotrophic compartment in the 50–100 m layer at equatorial station (TSS2). Data sources and calculations are as in Figure 2.

substantial daily dynamics, abundance and biomass levels of picophytoplankton populations are largely controlled by balanced grazing losses to microzooplankton [*Landry et al.*, 1997]. This had been inferred from previous diel studies of the picoplankton growth cycle [*Binder and DuRand*, 2002], but it has been difficult to confirm experimentally with simultaneous growth and grazing measurements [e.g., *Latasa et al.*, 1997; *Landry et al.*, 2000a]. The extreme photosensitivity and synchronous cell division cycle of *Prochlorococcus* spp. have presented particularly significant challenges for interpreting results of bottle incubations. In the present study, however, complementary assessments by pigment and populations gave relatively robust rate assessments consistent with those inferred from in situ observations [*Landry et al.*, 2003; *Neveux et al.*, 2003].

[24] The present analysis also shows that the balance applied broadly to the entire autotrophic community, with grazing accounting for 89–115% of total production depending on the calculation. This contrasts with the demonstrated importance of lateral advection during EqPac studies at 140°W in August–September 1992, where poleward transport of net phytoplankton production accounted for a 0.2 d^{-1} difference between growth and grazing losses to combined microplankton and mesozooplankton [*Landry et al.*, 1997]. Although EBENE was conducted during a comparable time of year and upwelling state, we saw no indication of the accumulation of large buoyant diatoms (*Rhizosolenia* spp.) at convergent fronts 2°–3° off the equator as they had during EqPac [*Yoder et al.*, 1994]. In this respect, EBENE results were more similar to the locally balanced state that existed at the equator during the El Niño phase of EqPac (February 1992) [*Landry et al.*, 1997]. Diatoms were a small fraction of total phytoplankton biomass, concentrated on the equator during EBENE [*Brown et al.*, 2003]. However, they had the most rapid turnover rates of all phytoplankton groups, implying high rates of silica remineralization.

[25] As shown in previous studies in the equatorial Pacific (on 140°W [*Dam et al.*, 1995]), mesozooplankton represent a relatively small, but important, component of total grazing because they feed disproportionately on the larger (>8 µm) particles [*Gaudy et al.*, 2003]. Such cells comprise about 21% of the autotrophic carbon, and our analysis suggests that the grazing by mesozooplankton is sufficiently high to utilize all of their production (Figure 2). Since microzooplankton also exert a considerable grazing impact on this larger size fraction, however, a substantial portion of the phytoplankton diet of mesozooplankton must come from the utilization of smaller cells, presumably larger cells among the <8-µm eukaryotes, or picoplankton consumed by larvaceans and pteropods. Nonetheless, the relatively low O:N (average atomic ratio = 6) ratio for mesozooplankton metabolism indicates protein catabolism, and the mesozooplankton:primary production ratio (0.08) places them between secondary and tertiary levels of the food web [*Gaudy et al.*, 2003]. These indices would seem to suggest that feeding on microzooplankton and predatory interactions within the mesozooplankton assemblage comprise more of the nutritional input to the mesozooplankton than direct consumption of phytoplankton.

6. Latitudinal Variations

[26] In comparing rate estimates between the time series stations, ^{14}C uptake was only slightly elevated at the equator (774 versus 699 mg C m^{-2} d^{-1}) while new

production was more than double that at 3°S (3.56 versus 1.40 mmol NO_3 m^{-2} d^{-1}) despite similar NO_3 availability [*Le Bouteiller et al.*, 2003]. The higher new production was consistent with more biogenic silica and faster Si uptake rates at the equator [*Leynaert et al.*, 2001], leading *Le Bouteiller et al.* [2003] to conclude that the upwelling supply rate of Si (and iron) to diatoms played a significant role in new production. According to the measurements made, siliceous organisms could account for as much as 69% of new production at the equator (TSS2), compared to 22% at TSS1.

[27] Latitudinal trends in community structure within the study region are reflected in various ratios of autotroph and grazer biomass based on the primary data by *Brown et al.* [2003] and *Le Borgne et al.* [2003]. Overall, little pattern can be seen in the biomass ratio of autotrophs to total grazers (microplankton + mesozooplankton) across the equatorial transect, most values falling within the range of ~ 1 to 2 (Figure 4b). At the extremes of the transect, however, the ratios are 2–3 times higher in subtropical waters of the South Pacific relative to those north of the equator. In addition, lower ratios of autotrophs to microzooplankton (Figure 4a) and mesozooplankton to microzooplankton (Figure 4c) indicate greater relative abundance of microzooplankton in waters on the northern side of the transect. Conversely, mesozooplankton were relatively more important on the southern side. These observations may be linked trophically, if, for example, grazing by the relatively high mesozooplankton biomass between 1°N and 7°S was responsible for reducing the concentration of heterotrophic protists. Reduced abundance, and therefore grazing pressure by protists, would help to explain, in turn, the higher concentrations of autotrophic and heterotrophic bacteria in the same region [*Brown et al.*, 2003]. North of the equator, the mesozooplankton biomass and therefore the feeding pressure on heterotrophic protists were presumably weaker, resulting in a higher biomass of small grazers. Relatively low biomass of all bacterial populations were found in this portion of the EBENE transect. Neither < 8 nor > 8-μm size categories of eukaryotic algae showed much response to the differences in grazer biomass distribution or asymmetry with respect to the equator. Thus, despite the latitudinal variations in grazers and picocyanobacterial populations, the total biomass of autotrophs was highest at the equator, the source of new iron and silicate input from upwelling, and only slightly asymmetrically distributed to the south.

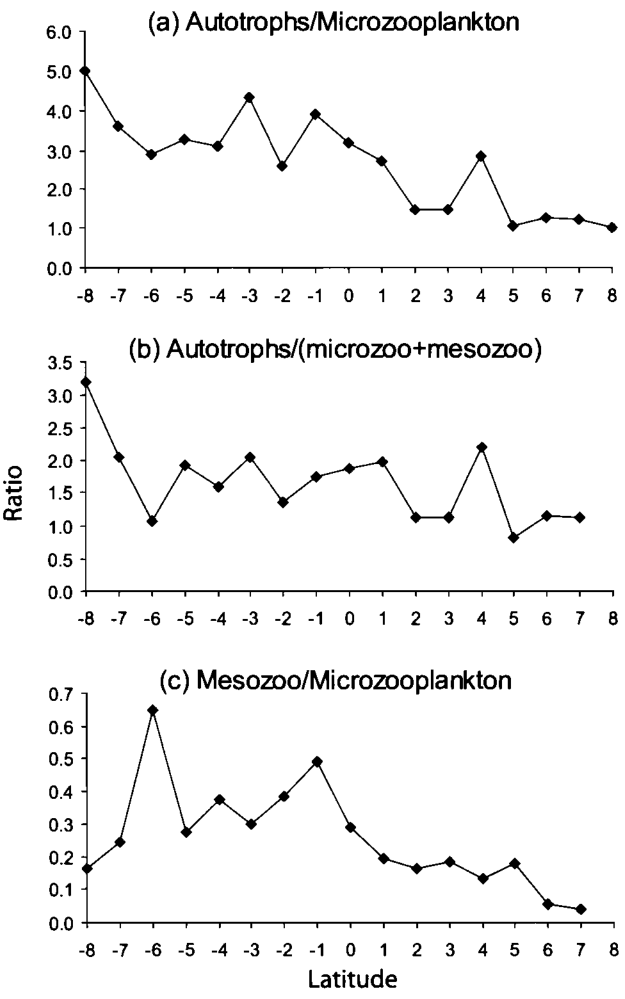

Figure 4. Carbon biomass ratios for different components of the 0–100 m plankton community along the EBENE transect. Autotrophs and microzooplankton are from *Brown et al.* [2003]; mesozooplankton are from *Le Borgne et al.* [2003].

[28] As a first-order attempt to resolve the latitudinal pattern in grazing pressure, we have applied the biomass-specific grazing functions derived from experimental studies at the equator (TSS2) to the biomass distributions of autotrophic and heterotrophic at each transect station. In effect, we assume that the main source of the grazing variability originates from the planktonic biomass and composition rather than from the rate estimates. For the major autotrophic taxa (Figure 5a), their respective grazing losses are equal to their mean carbon biomass [*Brown et al.*, 2003] in the 0–50 m layer multiplied times the biomass-specific clearance rates of microplankton and mesozooplankton and their respective grazer biomasses in the same layer. The biomass-specific clearance rate of the microzooplankton is equal to their mean grazing rate at 30 m (i.e., 0.56 d^{-1}) [*Landry et al.*, 2003] divided by the corresponding biomass at TSS2, which gives 0.053 m^3 $(mgC)^{-1}$ d^{-1}. The biomass-specific clearance rate of the mesozooplankton (0.031 m^3 $(mgC)^{-1}$ d^{-1}) was determined as described above. The microzooplankton biomass at a station is the sum of the protist [*Brown et al.*, 2003] and micrometazoan (<200 μm) standing stocks. The latter was estimated from the mesozooplankton biomass of *Le Borgne et al.* [2003], assuming that the smaller size fraction represents 17% of the mesozooplankton [*Le Borgne and Rodier*, 1997]. The mesozooplankton biomass only refers to suspension-feeding taxa, and it is therefore less than the total biomass at each station [from *Le Borgne et al.*, 2003]. Finally, while grazing losses to microzooplankton could be applied to all phytoplankton groups according to dilution assay results, the mesozooplankton were only assumed to consume > 8-μm autotrophs, following *Gaudy et al.* [2003]. According to these calculations, two phytoplankton groups account for most of the production lost to grazing, picoeukaryotes (33.6%) and *Prochlorococcus* (30.6%) (Figure 5a). Thus it is not surprising that microzooplankton account for

most of the grazing along the transect line (Figure 5b), as they did by direct measurement at the equator (Figure 2). Nonetheless, as the biomass ratios (Figure 4) suggest, the grazing contribution of microzooplankton is depressed south of 1°N (59–79%) compared to that from 1°N to 8°N (83–98%). Also notable from this analysis is a significant flux of production through the larger (>8-µm) algae, typically 20–40% of total grazing. This is mostly in the form of dinoflagellates and "other" categories (principally prymnesiophytes), and very little from diatoms. As noted previously (Figures 2 and 3), microzooplankton are significant consumers of this size fraction, in addition to their dominant role as grazers on picoplankton.

[29] As a cross-check on the relative magnitudes of the grazing impacts inferred from the calculation scheme described above, we compared these grazing estimates to the entirely independent data derived from ^{14}C uptake rates on 20-m water collected at each station and incubated under similar shipboard conditions [*Le Bouteiller et al.*, 2003]. These conditions were meant to simulate the light levels at 20 m, which was the depth of the photosynthesis maximum at the two time series stations. On a per volume basis, the 20-m production rates overestimate the mean rate for the 0–50 m layer by ~13% at TSS1 and 21% at TSS2. The effect is likely more modest (~5% according to data from R. Barber in the EqPac database; http://www.usjgofs.whoi.edu) for oligotrophic stations at the northern and southern ends of the transect, where the depth of the ^{14}C uptake maximum is deeper. On the other hand, we would also expect ^{14}C uptake rates to underestimate true phytoplankton biomass production by 10% or so, to reflect the effects of grazing and microbial cycling during the 12-hour incubations [*Laws et al.*, 2000]. Thus, on balance, these errors tend to offset one another.

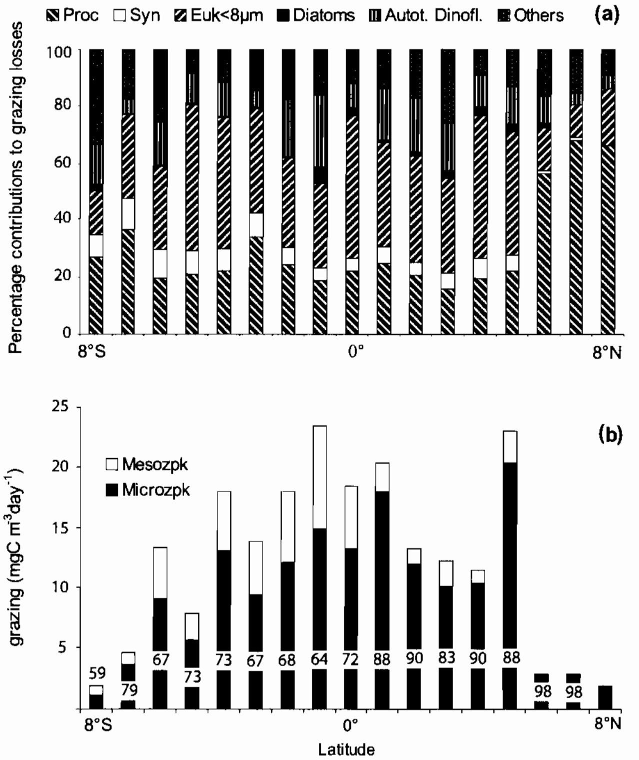

Figure 5. (a) Mean grazing losses of major autotrophic taxa in the 0–50 m layer along the EBENE transect (see text for data sources and calculations). (b) Grazing losses due to the microzooplankton (<200 µm) and mesozooplankton (200–2000 µm). Numbers refer to the percentage contribution of the microzooplankton to total grazing.

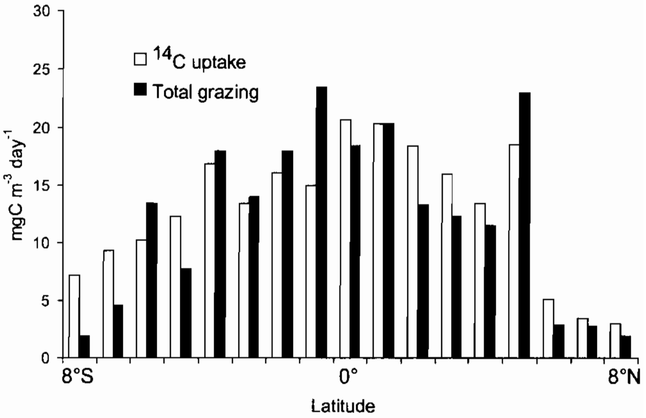

Figure 6. Comparison of ^{14}C uptake values at 20 m [from *Le Bouteiller et al.*, 2003] to the mean grazing estimates for the 0–50 m layer (Figure 5b) along the EBENE transect.

[30] There are many potential sources of error in this rate comparison, including sampling variability from one station to another, application of TSS2 rate values to other stations, the diversity of methods (^{14}C uptake, micrograzing rates from the dilution technique, mesozooplankton grazing from gut pigments, cell counts converted into carbon units). Nonetheless, the general patterns of production and grazing in Figure 6 show remarkable coherence throughout the transect region, though somewhat less so on the two most southern stations. The transect mean grazing estimate of 12.2 mgC m^{-3} d^{-1} is also close to that for production (12.8 mgC m^{-3} d^{-1}), implying a strong coupling of production and grazing processes throughout the region. At the equator (TSS2), the balance is more strongly constrained by relevant rate and biomass measurements from the same place and time (Figures 2 and 3). At least in the present study, however, the plankton community was sufficiently similar across the transect to allow broad application of rate inferences from detailed experimental results at the one central station. While it was not our *a priori* expectation that this would be so, the extent to which the diverse and independent methodologies show agreement for specific interactions at the equator as well as broad applicability across the transitions from HNLC to oligotrophic regimes suggests that the essential features of the system have been adequately represented.

[31] **Acknowledgments.** We gratefully acknowledge Gilles Tredunit, captain of the R/V *L'Atalante*, his crew, and the many shipmates and colleagues who facilitated and contributed to the success of the EBENE cruise. MRL was supported in part by NSF grants OCE-9218152, -9617409 and -9911765 as well as travel and logistical support from the IRD Centre de Noumea. This paper is contribution 976 from the U.S. JGOFS Program

and 6241 from the School of Ocean and Earth Science and Technology, University of Hawaii at Manoa, Honolulu, USA.

References

Azam, F., T. Fenchel, J. G. Gray, L. A. Meyer-Reil, and T. Thingstad, The ecological role of water-column microbes in the sea, *Mar. Ecol. Prog. Ser.*, *10*, 257–263, 1983.

Binder, B. J., and M. D. DuRand, Diel cycles in surface waters of the equatorial Pacific, *Deep Sea Res., Part II*, *49*, 2601–2617, 2002.

Blain, S., A. Leynaert, P. Treguer, M. J. Chretiennot-Dinet, and M. Rodier, Biomass, growth rates and limitation of equatorial Pacific diatoms, *Deep Sea Res., Part I*, *44*, 1255–1275, 1997.

Brown, S. L., M. R. Landry, J. Neveux, and C. Dupouy, Microbial community abundance and biomass along a 180° transect in the equatorial Pacific during an El Niño-Southern Oscillation cold phase, *J. Geophys. Res.*, *108*(C12), 8139, doi:10.1029/2001JC000817, in press, 2003.

Chai, F., R. C. Dugdale, T.-H. Peng, F. P. Wilkerson, and R. T. Barber, One dimensional ecosystem model of the equatorial Pacific upwelling system, part 1: Model development and silicon and nitrogen cycle, *Deep Sea Res., Part II*, *49*, 2713–2745, 2002.

Champalbert, G., J. Neveux, R. Gaudy, and R. Le Borgne, Diel variations of copepod feeding and grazing impact in the high-nutrient, low-chlorophyll zone of the equatorial Pacific Ocean (0°; 3°S, 180°), *J. Geophys. Res.*, *108*(C12), 8145, doi:10.1029/2001JC000810, in press, 2003.

Chavez, F. P., and J. R. Toggweiler, Physical estimates of global new production: The upwelling contribution, in *Upwelling in the Ocean: Modern Processes and Ancient Records*, edited by C. P. Summerhayes et al., pp. 313–320, John Wiley, Hoboken, N. J., 1995.

Chisholm, S. W., R. J. Olson, E. R. Zettler, J. Waterbury, R. Georicke, and N. Welshmeyer, A novel free-living prochlorophyte occurs at high concentrations in the oceanic euphotic zone, *Nature*, *334*, 340–343, 1988.

Coale, K. H., et al., A massive phytoplankton bloom induced by an ecosystem scale iron fertilization experiment in the equatorial Pacific Ocean, *Nature*, *383*, 495–501, 1996.

Cullen, J. J., M. R. Lewis, C. O. Davis, and R. T. Barber, Photosynthetic characteristics and estimated growth rates is the proximate control of primary production in the equatorial Pacific, *J. Geophys. Res.*, *97*, 639–654, 1992.

Dam, H. G., X. Zhang, M. Butler, and M. R. Roman, Mesozooplankton grazing and metabolism at the equator in the central Pacific: Implications for carbon and nitrogen fluxes, *Deep Sea Res., Part II*, *42*, 735–755, 1995.

Deibel, D., and S. H. Lee, Retention efficiency of sub-micrometer particles by the pharyngeal filter of the pelagic tunicate Oïkopleura vanhoeffeni, *Mar. Ecol. Prog. Ser.*, *81*, 25–30, 1992.

Dugdale, R. C., and F. P. Wilkerson, Silicate regulation of new production in the equatorial Pacific upwelling, *Nature*, *391*, 270–273, 1998.

Dupouy, C., H. Loisel, J. Neveux, S. L. Brown, C. Moulin, J. Blanchot, A. Le Bouteiller, and M. R. Landry, Microbial absorption and backscattering coefficients from in situ and POLDER satellite data during an El Niño-Southern Oscillation cold phase in the equatorial Pacific (180°), *J. Geophys. Res.*, *108*(C12), 8138, doi:10.1029/2001JC001298, in press, 2003.

Eldin, G., and M. Rodier, Ocean physics and nutrient fields along 180° during an El Niño-Southern Oscillation cold phase, *J. Geophys. Res.*, *108*(C12), 8137, doi:10.1029/2000JC000746, in press, 2003.

Feely, R. A., Seasonal and interannual variability of CO_2 in the equatorial Pacific, *Deep Sea Res., Part II*, *49*, 2443–2469, 2002.

Foley, D. G., T. D. Dickey, M. J. McPhaden, R. R. Bidigare, M. R. Lewis, R. T. Barber, S. T. Lindley, C. Garside, D. V. Manov, and J. D. McNeil, Longwaves and primary productivity variations in the equatorial Pacific at 0°, 140°W, *Deep Sea Res., Part II*, *44*, 1801–1826, 1997.

Friedrichs, M. A. M., and E. E. Hofmann, Physical control of biological processes in the central equatorial Pacific Ocean, *Deep Sea Res., Part I*, *48*, 1023–1069, 2001.

Frost, B. W., and N. C. Franzen, Grazing and iron limitation in the control of phytoplankton stock and nutrient concentration: A chemostat analogue of the equatorial upwelling zone, *Mar. Ecol. Prog. Ser.*, *83*, 291–303, 1992.

Gaudy, R., G. Champalbert, and R. Le Borgne, Feeding and metabolism of mesozooplankton in the equatorial Pacific high-nutrient, low-chlorophyll zone along 180°, *J. Geophys. Res.*, *108*(C12), 8144, doi:10.1029/2000JC000743, in press, 2003.

Gordon, R. M., K. H. Coale, and K. S. Johnson, Iron distributions in the equatorial Pacific: Implications for new production, *Limnol. Oceanogr.*, *141*, 419–431, 1997.

Gorsky, G., M. J. Chrétiennot-Dinet, J. Blanchot, and I. Palazzoli, Picoplankton and nanoplankton aggregation by appendicularians: Fecal pellet contents of *Megalocercus huxleyi* in the equatorial Pacific, *J. Geophys. Res.*, *104*, 3381–3390, 1999.

Gorsky, G., R. Le Borgne, M. Picheral, and L. Stemmann, Marine snow latitudinal distribution in the equatorial Pacific along 180°, *J. Geophys. Res.*, *108*(C12), 8146, doi:10.1029/2001JC001064, in press, 2003.

Hutchins, D. A., and K. W. Bruland, Iron-limited diatom growth and Si:N uptake ratios in a coastal upwelling regime, *Nature*, *393*, 561–564, 1998.

Landry, M. R., et al., Iron and grazing constraints on primary production in the central equatorial Pacific: An EqPac synthesis, *Limnol. Oceanogr.*, *42*, 405–418, 1997.

Landry, M. R., J. Constantinou, M. Latasa, S. L. Brown, R. R. Bidigare, and M. E. Ondrusek, Biological response to iron fertilization in the eastern equatorial Pacific (IronEx II). III. Dynamics of phytoplankton growth and microzooplankton grazing, *Mar. Ecol. Prog. Ser.*, *201*, 57–72, 2000a.

Landry, M. R., M. E. Ondrusek, S. J. Tanner, S. L. Brown, J. Constantinou, R. R. Bidigare, K. H. Coale, and S. Fitzwater, Biological response to iron fertilization in the eastern equatorial Pacific (IronEx II). I. Microplankton community abundances and biomass, *Mar. Ecol. Prog. Ser.*, *201*, 27–42, 2000b.

Landry, M. R., S. L. Brown, J. Neveux, C. Dupouy, J. Blanchot, S. Christensen, and R. R. Bidigare, Phytoplankton growth and microzooplankton grazing in high-nutrient, low-chlorophyll waters of the equatorial Pacific: Community and taxon-specific rate assessments from pigment and flow cytometric analyses, *J. Geophys. Res.*, *108*(C12), 8142, doi:10.1029/2000JC000744, in press, 2003.

Latasa, M., M. R. Landry, L. Schlüter, and R. R. Bidigare, Pigment-specific growth and grazing rates of phytoplankton in the central equatorial Pacific, *Limnol. Oceanogr.*, *42*, 289–298, 1997.

Laws, E. A., M. R. Landry, R. T. Barber, L. Campbell, M.-L. Dickson, and J. Marra, Carbon cycling in primary production bottle incubations: Inferences from grazing experiments and photosynthetic studies using ^{14}C and ^{18}O in the Arabian Sea, *Deep Sea Res., Part II*, *47*, 1339–1352, 2000.

Le Borgne, R., Campagne océanographique EBENE à bord du N. O. *L'Atalante* 21 Octobre au 20 Novembre 1996. Recueil de données. Tome 2: Matière organique, pigments photosynthétiques, production primaire, micro-et mésozooplancton, profileur vidéo marin, *Arch. Sci. Mer Oceanogr. Phys. Cent. Noumea ORSTOM*, *4*, 187 pp., 1999.

Le Borgne, R., and M. Rodier, Net zooplankton and the biological pump: A comparison between the oligotrophic and mesotrophic equatorial Pacific, *Deep Sea Res., Part II*, *44*, 2003–2023, 1997.

Le Borgne, R., M. J. Langlade, P. Polidori, and M. Rodier, Campagne océanographique EBENE à bord du N. O. *L'Atalante* 21 Octobre au 20 Novembre 1996. Recueil de données. Tome 1: Météorologie, courantologie, données de surface, hydrologie,sels nutritifs et phytoplankton, *Arch. Sci. Mer Oceanogr. Phys. Cent. Noumea ORSTOM*, *1*, 363 pp., 1998.

Le Borgne, R., R. T. Barber, T. Delcroix, H. Y. Inoue, D. J. Mackey, and M. Rodier, Pacific warm pool and divergence: Temporal and zonal variations on the equator and their effects on the biological pump, *Deep Sea Res., Part II*, *49*, 2471–2512, 2002a.

Le Borgne, R., R. A. Feely, and D. J. Mackey, Carbon fluxes in the equatorial Pacific: A synthesis of the JGOFS programme, *Deep Sea Res., Part II*, *49*, 2425–2442, 2002b.

Le Borgne, R., G. Champalbert, and R. Gaudy, Mesozooplankton biomass and composition in the equatorial Pacific along 180°, *J. Geophys. Res.*, *108*(C12), 8143, doi:10.1029/2000JC000745, 2003.

Le Bouteiller, A., A. Leynaert, M. Landry, R. Le Borgne, J. Neveux, M. Rodier, J. Blanchot, and S. Brown, Primary production, new production, and growth rate in the equatorial Pacific: Changes from mesotrophic to oligotrophic regime, *J. Geophys. Res.*, *108*(C12), 8141, doi:10.1029/2000JC000914, in press, 2003.

Leonard, C. L., C. R. McClain, R. Murtugudde, E. E. Hofmann, and L. W. Harding Jr., An iron based ecosystem model of the central equatorial Pacific, *J. Geophys. Res.*, *104*, 1325–1341, 1999.

Leynaert, A., P. Tréguer, C. Lancelot, and M. Rodier, Silicon limitation of biogenic silica production in the equatorial Pacific, *Deep Sea Res., Part I*, *48*, 639–660, 2001.

Minas, H. J., M. Minas, and T. T. Packard, Productivity in upwelling areas deduced from hydrographic and chemical fields, *Limnol. Oceanogr.*, *31*, 1182–1206, 1986.

Morel, F. M., J. G. Rueter, and N. M. Price, Iron nutrition of phytoplankton and its possible importance in the ecology of open ocean regions with high nutrient and low biomass, *Oceanography*, *4*, 56–61, 1991.

Murray, J. W., E. Johnson, and C. Garside, A U.S. JGOFS Process Study in the equatorial Pacific (EqPac): Introduction, *Deep Sea Res., Part II*, *42*, 275–293, 1995.

Neveux, J., C. Dupouy, J. Blanchot, A. Le Bouteiller, M. R. Landry, and S. L. Brown, Diel dynamics of chlorophylls in high-nutrient, low-chlorophyll waters of the equatorial Pacific (180°): Interactions of growth, grazing, physiological responses, and mixing, *J. Geophys. Res.*, *108*(C12), 8140, doi:10.1029/2000JC000747, in press, 2003.

Price, N. M., B. A. Ahner, and F. M. M. Morel, The equatorial Pacific Ocean: Grazer controlled phytoplankton populations in an iron-limited ecosystem, *Limnol. Oceanogr.*, *39*, 520–534, 1994.

Roman, M. R., H. G. Dam, A. L. Gauzens, J. Urban-Rich, D. G. Foley, and T. D. Dickey, Zooplankton variability on the equator at 140°W during the JGOFS EqPac study, *Deep Sea Res., Part II*, *42*, 673–693, 1995.

Turner, J. T., The feeding ecology of some zooplankters that are important prey items of larval fish, *NOAA Tech. Rep. NMFS 7*, 28 pp., Natl. Oceanic and Atmos. Admin., Silver Spring, Md., 1984.

Walsh, J. J., Herbivory as a factor in patterns of nutrient utilization in the sea, *Limnol. Oceanogr.*, *21*, 1–13, 1976.

White, J. R., X. Zhang, L. A. Welling, M. R. Roman, and H. G. Dam, Latitudinal gradients in zooplankton biomass in the tropical Pacific at 140°W during the JGOFS EqPac study: Effects of El Niño, *Deep Sea Res., Part II*, *42*, 715–733, 1995.

Yoder, J. A., S. G. Ackelson, R. T. Barber, P. Flament, and W. M. Balch, A line in the sea, *Nature*, *371*, 689–692, 1994.

M. R. Landry, Department of Oceanography, University of Hawaii at Manoa, 1000 Pope Rd., Honolulu, HI 96822, USA.

R. Le Borgne, Centre IRD, B.P. A5, Nouméa Cédex, New Caledonia. (leborgne@noumea.ird.nc)

Le Borgne Robert, Landry M.R. (2003).

EBENE : a JGOFS investigation of plankton variability and trophic interactions in the equatorial Pacific (180°).

In : A JGOFS investigation of plankton variability and trophic interactions in the central equatorial Pacific (EBENE).

Journal of Geophysical Research, 108 (C12), 1-1 - 1-10. ISSN 0148-0227